Limits of time–delayed feedback control

Wolfram Just [a,1], Ekkehard Reibold [b,2], Hartmut Benner [b], Krzysztof Kacperski [a,c,b], Piotr Fronczak [c], and Janusz Hołyst [c,b,a,3]

[a] *Max Planck Institute for Physics of Complex Systems, Nöthnitzer Straße 38, D–01187 Dresden, Germany*

[b] *Institut für Festkörperphysik, Technische Universität Darmstadt, Hochschulstraße 6, D–64289 Darmstadt, Germany*

[c] *Institute of Physics, Warsaw University of Technology, Koszykowa 75, PL–00–662 Warsaw, Poland*

Abstract

General features of stability domains for time–delayed feedback control exist, which can be predicted analytically. We clarify, why the control scheme with a single delay term can only stabilise orbits with short periods or small Lyapunov exponents, and derive a quantitative estimate. The limitation can be relaxed by employing multiple delay terms. In particular, the extended time delay autosynchronisation method is investigated in detail. Analytic calculations are in good agreement with results of numerical simulations and with experimental data from a nonlinear diode resonator.

Keywords: Chaos control, Pyragas method, Differential–difference equation

1 Introduction

Controlling the motion of dynamical systems is one of the classical subjects in engineering and mathematical science. Sophisticated tools have been developed for that purpose (cf. e. g. [1]). Within the last decade such topics have attracted the interest of many physicists in the context of nonlinear dynamics since the potentially large number of unstable periodic orbits which are embedded in chaotic attractors opens the possibility to stabilise different states with

[1] e–mail: wolfram@mpipks-dresden.mpg.de

[2] e–mail: Ekkehard.Reibold@physik.tu-darmstadt.de

[3] e–mail: jholyst@if.pw.edu.pl

very small control power. A conceptually quite simple method which avoids fancy data processing and is based solely on the plain measurement and the time lag of a scalar signal has been proposed by Pyragas [2]. Despite the large amount of simulations and numerical analyses (cf. e. g. [3–6]) and several real experimental realisations (cf. [7,8]) little is known from the theoretical and systematic point of view. Some progress has been made in understanding topological constraints of the control scheme [9,10] and the adaptation of delay times [11] from a systematic point of view. Here, we are concerned with the frequent numerical observation that the original Pyragas method using a single delay time is limited to orbits with short periods or small Lyapunov exponents. To overcome such limitations extended delay schemes have been proposed [5], but a deeper theoretical explanation is still missing.

2 Theoretical analysis

Following the lines of [9] we start with a fairly general dynamical equation which is subjected to a control force F,

$$\dot{\boldsymbol{x}} = \boldsymbol{f}(\boldsymbol{x}(t), F(t)) \quad . \tag{1}$$

We presuppose that without control, $F \equiv 0$, the system admits an unstable periodic orbit $\boldsymbol{\xi}(t) = \boldsymbol{\xi}(t+\tau)$ with Floquet exponents $\lambda_\ell + i\omega_\ell$. At least one exponent has positive real part, $\lambda > 0$. In what follows we concentrate on such a branch and, therefore, suppress the subscript. The force aims at stabilising the orbit $\boldsymbol{\xi}$. Using the basic idea of delayed feedback control an appropriate force can be derived simply from the measurement of a scalar quantity $g[\boldsymbol{x}(t)]$

$$F(t) := K \sum_{\nu=0}^{\infty} s_\nu \left\{ g[\boldsymbol{x}(t-\nu\tau)] - g[\boldsymbol{x}(t-(\nu+1)\tau)] \right\} \quad . \tag{2}$$

Such a construction ensures that the periodic orbit remains a genuine orbit of the system subjected to the control. The original method proposed by Pyragas corresponds to the choice $s_\nu = \delta_{\nu,0}$, whereas more general concepts like the extended time delay autosynchronisation [5] are also included by $s_\nu = R^\nu$. For convenience K denotes the control amplitude.

The stability of the periodic orbit is computed from the ordinary linear stability analysis according to $\boldsymbol{x}(t) = \boldsymbol{\xi}(t) + \delta\boldsymbol{x}(t)$. If we take into account that owing to the periodic time dependencies Floquet theory can be applied [12], i. e. $\delta\boldsymbol{x}(t) = \exp[(\Lambda + i\Omega)t]\boldsymbol{v}(t)$ holds with Floquet exponent $\Lambda + i\Omega$ and periodic eigenvectors $\boldsymbol{v}(t) = \boldsymbol{v}(t+\tau)$, we end up with

$$\Lambda + i\Omega = \Gamma \left[K \left\{ 1 - \exp[-(\Lambda + i\Omega)\tau] \right\} \sum_{\nu=0}^{\infty} s_\nu \exp[-\nu(\Lambda + i\Omega)\tau] \right] \quad . \tag{3}$$

The whole details of the system enter via a function Γ which itself is a Floquet exponent determined by the linear stability of the uncontrolled orbit and the control matrix [9]. In particular $\Gamma[0] = \lambda + i\omega$ holds, Γ is piecewise analytic and increases at most linearly with its argument. As pointed out previously, a finite torsion is a necessary constraint for delayed feedback methods to work at all (cf. [10] for some rigorous statements). Hence we restrict ourselves to the simplest case which is frequently met in low–dimensional systems for topological reasons. We suppose namely that the neighbourhood of the orbit flips during one turn, i. e. $\omega = \pi/\tau$. In order to get quantitative results we perform a Taylor series expansion of eq.(3). Such an expansion can be performed at an arbitrary real value of the argument of Γ. We obtain at first order, introducing dimensionless quantities,

$$P + i\Phi = p - x\,(1 + \exp[-P - i\Phi]) \sum_{\nu=0}^{\infty} (-1)^{\nu} s_{\nu} \exp[-(P + i\Phi)\nu] \quad . \qquad (4)$$

Here $P = \Lambda\tau$ denotes the Lyapunov exponent of the orbit subjected to control in units of the period, $\Phi = \Omega\tau - \pi$ the deviation of the frequency, $x = (-\tau\chi')K$ the rescaled control amplitude, and χ' the real first Taylor series coefficient of Γ. If the expansion is performed around zero, then $p = \Gamma[0]\tau - i\pi$ formally coincides with the Lyapunov exponent of the free orbit, $\lambda\tau$. For a different expansion point the value of p represents at least a first order estimate for $\lambda\tau$. Henceforth we will identify p with the Lyapunov exponent of the free orbit. Both quantities, χ' as well as p, depend explicitly on the details of the system and may be considered as fit parameters. One might object that the approximation employed in eq.(4) is too crude for studying real control properties. However, it has turned out that several features can be predicted quite well even quantitatively [9,3].

Let us first recall the original Pyragas scheme, $s_0 = 1$, $s_{\nu\geq 1} = 0$. For a given orbit the region of stability, i. e. the parameter interval in x where eq.(4) admits only solutions with $P < 0$, is typically bounded by two points. At the lower boundary the real part Λ changes sign from positive to negative values with a frequency $\Omega = \omega = \pi/\tau$, ($\Phi = 0$), i. e. a flip bifurcation occurs. On increasing the control amplitude the stable eigenvalue branch collides with an additional exponent giving rise to a finite frequency deviation $\Phi \neq 0$. The corresponding real part increases again and changes sign at the upper bound of the stability interval causing a Hopf bifurcation. Both critical values are easily evaluated from eq.(4) as

$$x^{(\mathrm{fl})} = p/2 \qquad (5)$$

and

$$x^{(\mathrm{ho})} = \Phi/\sin\Phi, \quad p = \Phi/\tan(\Phi/2), \quad (\Phi \in [0, \pi]) \quad , \qquad (6)$$

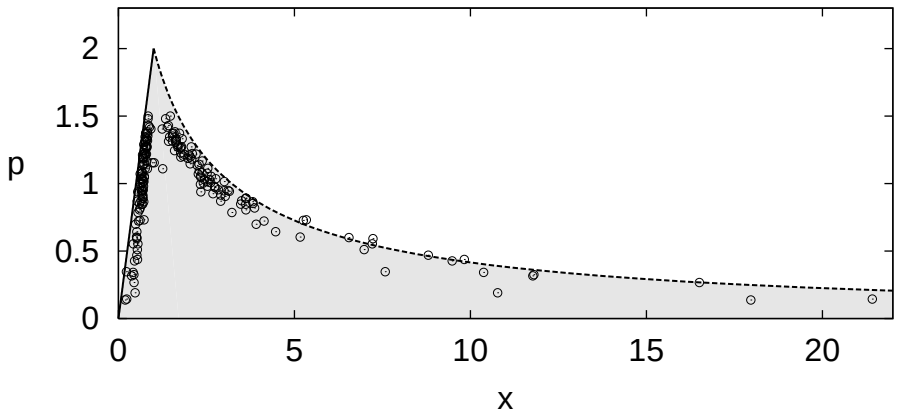

Fig. 1. Stability domain for ordinary Pyragas control in the parameter plane of rescaled control amplitude x and Lyapunov exponent p (greyshaded). The solid/dashed line indicates the flip/Hopf instability (eq.(5)/(6)). Symbols are results of simulations for the Rössler model with different parameter settings.

where the second expression gives the parametric representation of the boundary in the x–p plane. Fig. 1 displays these boundaries in the parameter plane. Although analytical calculations of such boundaries for fixed points of the corresponding delay systems are well established (e. g. [13]) and have been performed for particular maps and differential equations [6] less has been known about limit cycles. Here, we stress the fact that within our approximation orbits with $p > 2$ cannot be stabilised at all. It is remarkable that this critical value does not depend on the system parameter χ'. Altogether our findings explain to some extent the frequent numerical observation that orbits with large periods or highly unstable orbits cannot be stabilised by the original Pyragas approach with a single delay term.

Let us illustrate this analytical result with numerical simulations of the Rössler model, $\dot{x}_1 = -x_2 - x_3$, $\dot{x}_2 = x_1 + ax_2$, $\dot{x}_3 = b + x_1x_3 - cx_3$. Using $g[\boldsymbol{x}] = x_2$ we have subtracted the control force (2) with $s_\nu = \delta_{\nu,0}$ from the right hand side of the second equation. For control purpose we have focused on the period–one orbit with respect to the canonical Poincaré surface of section $x_1 = x_2$. Parameters have been chosen randomly from the cube $a \in [0.15, 0.35]$, $b \in [0.1, 0.8]$ and $c \in [3, 8]$. For 100 parameter combinations the minimal and maximal control amplitudes have been obtained from plain time series like in real experimental situations. In each parameter setting the delay time was adapted with a scheme similar to that proposed in [14]. The Lyapunov exponent of the orbit was estimated by observing the exponential escape from the orbit after switching off the control. The corresponding data points are displayed in Fig. 1. To obtain the rescaled control amplitude x the coefficient χ' has been calculated for each orbit using the point of maximal stability [9]. The coincidence between numerical data and the theoretical prediction is quite

convincing. Small deviations appear close to the critical value $p = 2$, since we have not found unstable periodic orbits with $p > 1.6$.

3 Extended control schemes

To overcome the limitations which are caused by the size of the Lyapunov exponent let us consider control schemes that employ multiple delay terms. For the purpose of illustration we begin with the simplest extension by taking only two delay terms into account, $s_0 = 1$, $s_1 \neq 0$, $s_{\nu \geq 2} = 0$. Now the control scheme admits three parameters, the Lyapunov exponent of the uncontrolled orbit p , the rescaled control amplitude x , and the relative weight of the additional control term s_1 . The stability boundaries are caused by the same mechanism already described above. For the boundary determined by the flip instability we obtain

$$x^{(\mathrm{fl})}(1 - s_1) = p/2 \quad , \tag{7}$$

whereas for the boundary generated by the Hopf instability eq.(4) leads to

$$\begin{aligned} x^{(\mathrm{ho})} &= \frac{p}{2}\frac{1 + 2\cos\Phi}{1 + \cos\Phi} - \frac{\Phi}{\sin\Phi}\frac{2\cos\Phi - 1}{2} \\ s_1 &= \frac{p\tan(\Phi/2) - \Phi}{p\tan(\Phi/2)(1 + 2\cos\Phi) - \Phi(2\cos\Phi - 1)}, \quad (\Phi \in [0, \pi]) \quad . \end{aligned} \tag{8}$$

Fig. 2 shows the stability region determined by these curves for three values of p. For $p > 2$ the stability region does not reach the x–axis, i. e. stabilisation is not achieved by the original Pyragas scheme. However, control is possible by employing the second delay term associated to the variable s_1. But even this method fails for $p > 4$ since the stability domain vanishes, as easily computed from eqs.(7) and (8).

To confirm the analytical results, eqs.(7) and (8), we used once more the Rössler model with parameter values $a = b = 0.2$ and $c = 5.7$. The control force was derived from the bounded quantity $g[\boldsymbol{x}] = \tanh[(x_1 + x_2)/10]$ and the force was coupled to the first and the second equation of motion. The stabilisation of the period–two orbit with period $\tau = 11.758\ldots$ was considered. Within a straightforward numerical simulation the domain in parameter space where stabilisation works successfully was explored, and the data are displayed in Fig. 2. Our data points are compared with the analytical results of eqs.(7) and (8), where the unknown parameters p and $(-\tau\chi')$ have been fixed appropriately. The almost perfect agreement confirms that the analytical results explain in the present case the main features not only qualitatively, but even quantitatively.

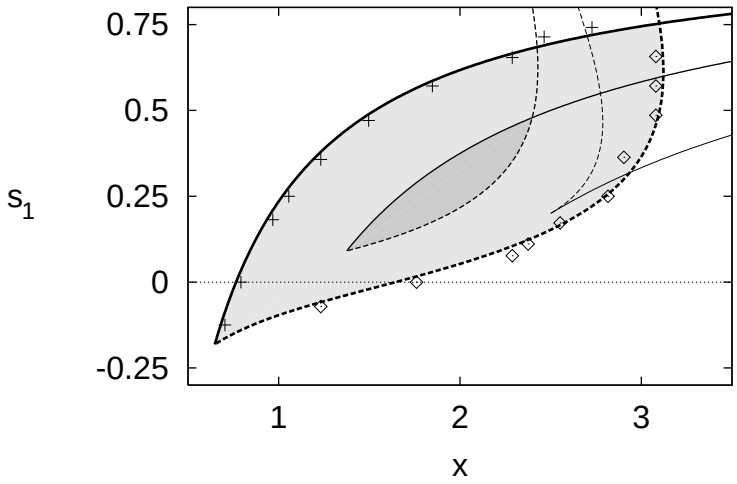

Fig. 2. Stability boundaries for two time control in the plane of rescaled control amplitude x and relative weight s_1. Solid/dashed lines indicate the flip/Hopf instability (eq.(7)/(8)). Thick lines correspond to $p = 1.53$ and medium lines to $p = 2.5$. The stability domains are shaded. In addition, the critical case $p = 4.0$ is shown by thin lines. Crosses/diamonds indicate the results for the flip/Hopf boundary obtained from a numerical simulation of the Rössler model using the values $p = 1.53$ and $(-\tau\chi') = 0.88$ for an optimal fit.

Our previous considerations clearly show that the inclusion of additional delay terms relaxes the constraint which originates from the size of the Lyapunov exponent. Unfortunately, realising control forces with a large number of independent delay terms becomes increasingly difficult. A very effective control scheme which uses the advantage of multiple delays but is easily implemented has been proposed in [5]. It corresponds to a geometrically decreasing sequence of weights in eq. (2), $s_\nu = R^\nu$, $|R| < 1$. According to eq.(4) the stability boundaries are obtained as

$$x^{(\mathrm{fl})}/(1+R) = p/2 \tag{9}$$

and

$$\begin{aligned} x^{(\mathrm{ho})} &= (p^2+\Phi^2)\frac{\tan(\Phi/2)}{\Phi + p\tan(\Phi/2)} \\ R &= \frac{p\tan(\Phi/2)-\Phi}{p\tan(\Phi/2)+\Phi}, \quad (\Phi \in [0,\pi]) \quad . \end{aligned} \tag{10}$$

Fig. 3 shows the stability region for several values of R in the x–p parameter plane as well as the stability region in the x–R control parameter plane for different values of the Lyapunov exponent p. For each value of p there exists a finite stability interval in x, at least if R is chosen sufficiently large. For fixed value of R the stability domains extend up to a maximal p–value $2(1+R)/(1-R)$, as easily computed from eqs.(9) and (10). By employing large R–values

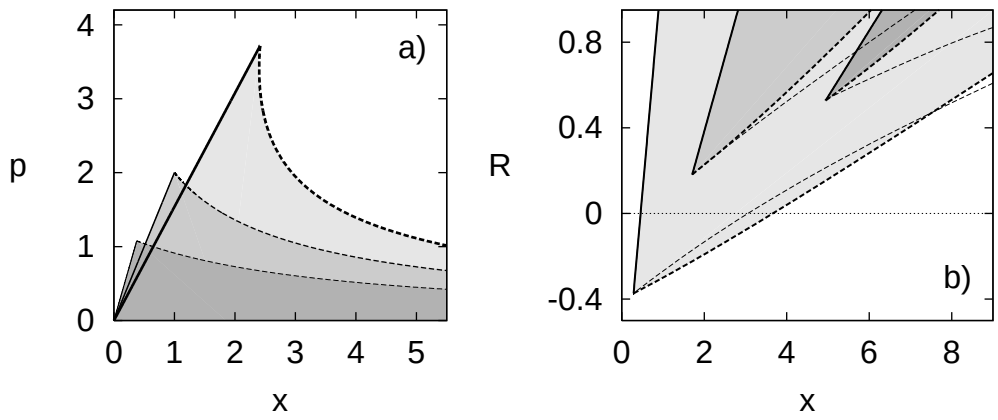

Fig. 3. Stability boundaries for extended time delay autosynchronisation : a) Parameter plane of rescaled control amplitude x and Lyapunov exponent p with $R = -0.3$ (thin lines), $R = 0.0$ (medium lines), and $R = 0.3$ (thick lines); b) x–R control parameter plane for three values of the Lyapunov exponent p (thick lines, from bottom to top $p = 0.91, 2.89, 6.47$). Solid/dashed lines indicate the flip/Hopf instability (eq.(9)/(10)), the stability domains are shaded. Thin lines in b) display the numerically "exact" Hopf boundaries for the period–one orbit in the Rössler equation at $a = 0.2, 0.6$, and 0.9 with fit parameters $(-\tau\chi') = 0.33, 0.55$, and 1.20 respectively (from bottom to top).

control can always be achieved within our approximation. In that sense the control scheme is superior to the ordinary Pyragas approach as claimed in [5]. However, it follows from the analytical expressions that the domain shrinks in size and shifts towards larger control amplitudes for increasing values of the Lyapunov exponent p. Our analytical findings are in agreement with the treatment of fixed points in two–dimensional systems [6].

As in the previous case of two time delay we use the Rössler model to illustrate our analytical result on extended control schemes. We concentrate on the stabilisation of the period–one orbit at parameter values $b = 0.2$ and $c = 5.7$. Parameter a is varied to realise orbits with different Lyapunov exponents. The stability boundaries within the K–R parameter plane can be computed "exactly" from the numerical solution of the linearised equation of motion. Such an approach needs only the integration of plain differential equations (cf. [15]). Results for three particular orbits, i. e. three particular system parameters, are displayed in Fig. 3b. We stress that, for appropriate values of the fit parameter $p/(-\tau\chi')$, the boundary caused by the flip instability coincides with the analytical expression, since eq.(9) is an exact consequence of the full eigenvalue equation (3) and valid beyond the first–order Taylor series truncation. The deviations which occur for the boundary caused by the Hopf instability can be attributed to such a simple approximation and hence are not at all surprising. However, the qualitative features are correctly reproduced. In addition, one should keep in mind that the exact Hopf boundary is difficult to observe

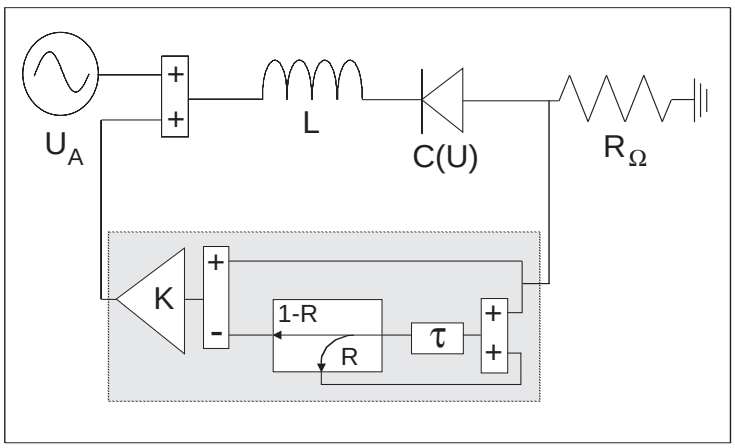

Fig. 4. Experimental setup of the nonlinear diode resonator with extended time delay feedback device.

in plain simulations. Stabilisation is unlikely to occur in the close vicinity of the transition line, because of finite basins of attraction and small real parts, Λ.

Altogether our simple analytical expression captures most of the essential features observed for the extended scheme. Last but not least, we mention that the analytical formulas (9) and (10) are again in reasonable agreement with the experimental data of [16].

4 Electronic circuit experiments

Let us finally present results of the experiments performed on a nonlinear diode resonator (cf. Fig. 4). The circuit, consisting of a diode (1N4005), an inductor (47 mH), and a resistor (36Ω), was sinusoidally driven at fixed frequency (800 kHz). Without control the system undergoes a period–doubling cascade into chaos on variation of the driving amplitude U_A. On further increase there occur periodic windows of period–2, 3, 4, and 5 which also undergo period–doubling cascades into chaos. Topological analysis [17] of this three–dimensional system yielded a frequency of π/τ in the Floquet exponent for the unstable period–1, 2, and 4 orbits of the chaotic attractor. This corresponds to a flip of the neighbourhood of these orbits. Therefore, the orbits are accessible to time–delayed feedback control.

The control device consists of a cascade of electronic delay lines with a limiting frequency of about 3MHz and several operational amplifiers acting as preamplifier, subtractor, or inverter. The device allows to apply a control force of the form $F(t) = -K[U(t) - (1-R)S(t-\tau)]$, $S(t) = U(t) + RS(t-\tau)$ which is equivalent to eq.(2) with $s_\nu = R^\nu$. Parameter ranges are $R = 0 \ldots 1$,

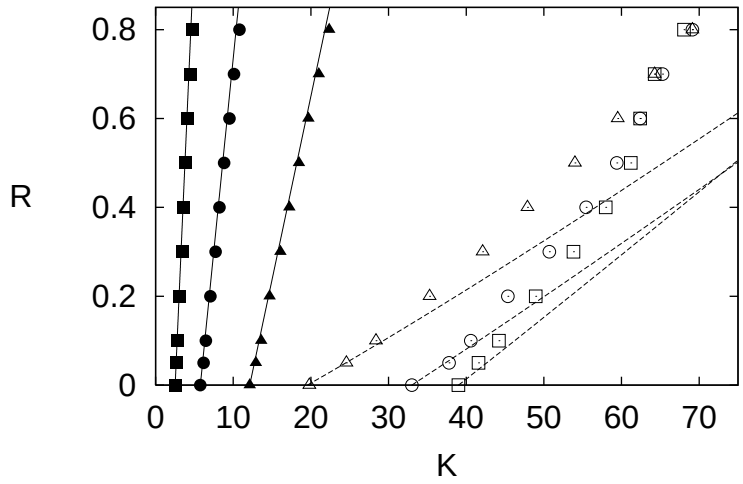

Fig. 5. Stability range in the K–R parameter plane for three values of the driving amplitude: □ 0.8V, ○ 1.1V, △ 3.5V. Full/open symbols corrspond to the flip/Hopf boundary. Solid/dashed lines indicate the analytical result (9)/(10) with fit parameters $[p;(-\tau\chi')] = [0.69;0.137]$ (0.8V), $[1.05;0.091]$ (1.1V), and $[1.70;0.070]$ (3.5V).

$\tau = 10\text{ns}\ldots 21\mu\text{s}$. Our feedback scheme consisted of coupling the voltage at the resistor via the control device to the driving force.

To check the coincidence with our analytical results for the simple and extended control algorithm we measured the range of control amplitudes for successful control of the period–one orbit and determined $K^{(\text{fl})}$ and $K^{(\text{ho})}$ in dependence on the control parameter R. The results for three different driving amplitudes are displayed in Fig. 5. The fit of the analytical result yields a perfect agreement for the flip boundary, for the reason already mentioned above. As expected, we observe slight deviations for the Hopf boundary since the analytical result is just a first–order approximation.

In addition, we measured the Lyapunov exponent of the free orbit, p, by observing the exponential increase of the control signal when the control is turned off. The frequency deviation Φ can be measured with high precision from the spectrum of the control signal at the Hopf boundary, whereas exponents p larger than one are difficult to evaluate from the experimental data. The experimental stability boundaries in the K–p parameter plane as well as the corresponding values of the frequency deviation are shown in Fig. 6. Although one observes a qualitative agreement with the corresponding analytical result (cf. Fig. 3a), a quantitative evaluation is difficult to perform. For each data point one has at least one fit parameter $(-\tau\chi')$ so that at this level no real comparison can be made. Fortunately eqs.(9) and (10) yield a relation between the two critical amplitudes $K^{(\text{fl})}$, $K^{(\text{ho})}$, the control parameter R, and the frequency deviation at the Hopf boundary Φ which does not contain any

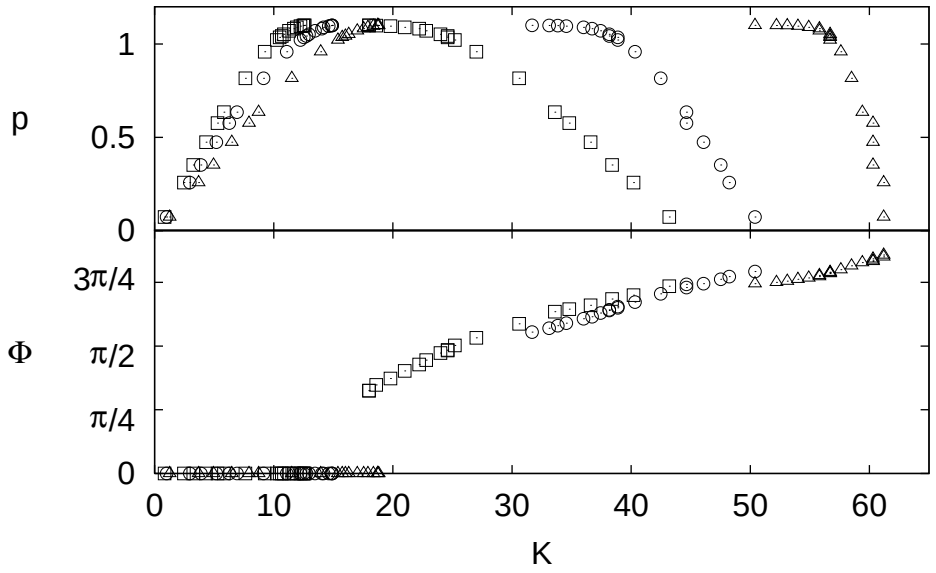

Fig. 6. Stability boundaries in the K–p plane for the period–one orbit and corresponding frequency deviation Φ for three values of R: $\Box$ ($R = 0$), $\circ$ ($R = 0.2$), and $\triangle$ ($R = 0.5$) obtained from the transient dynamics in the electronic circuit experiment.

system parameter

$$\frac{K^{(\mathrm{fl})}}{K^{(\mathrm{ho})}} = 1 \Big/ \left[1 + \left(\frac{1-R}{1+R}\tan\frac{\Phi}{2}\right)^2\right] \quad . \tag{11}$$

Although we could already compare this expression with the data presented in Fig. 6, the accessible range of frequency deviations is too small for meaningful results. Therefore we concentrate on control of the period-4 orbit and the corresponding data are shown in Fig. 7. In view of the fact that the analytical curves do not contain any fit parameter the coincidence is remarkable. Hence, we conclude that already the first order analytical expression contains the essential qualitative and several quantitative features which determine the stability domain for feedback control.

5 Conclusion

In conclusion, our analytical approach, which was based on a first–order series expansion in the control amplitude has shown that the collision of eigenvalues resulting in a finite frequency deviation limits the success of time–delayed feedback control. Within our approximation the original Pyragas scheme is limited to orbits with short periods or small Lyapunov exponents such that

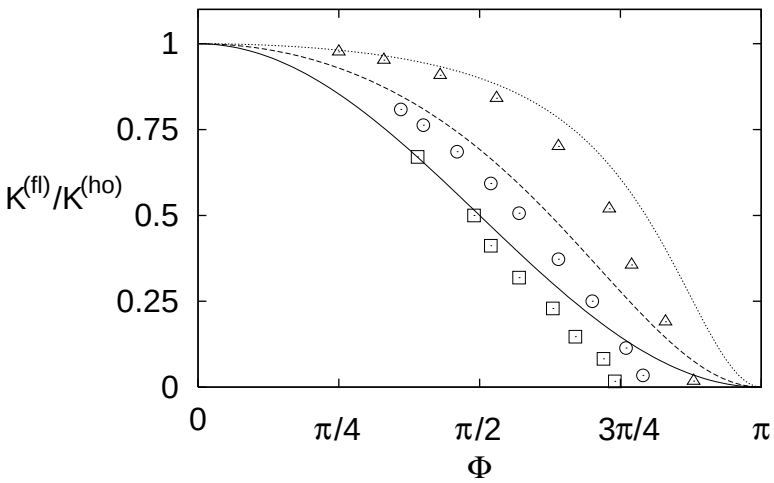

Fig. 7. Ratio of critical control amplitudes in dependence on the frequency deviation Φ at the Hopf instability for several values of R. Symbols are results of the electronic circuit experiment, lines display the analytical expression (11): $R = 0$ ($\Box$, solid line), $R = 0.2$ ($\circ$, dashed line), and $R = 0.5$ ($\triangle$, dotted line).

$\lambda\tau < 2$. The limitation can be overcome by taking multiple delays into account. The inclusion of two delay terms relaxes the condition to $\lambda\tau < 4$, while for the extended time delay autosynchronisation in principle no constraint is obtained at this level. For all schemes there are limited ranges of the control amplitude K that can be employed to stabilise the desired periodic orbit, and orbits with large values of the exponent $\lambda\tau$ can be stabilised only in very limited ranges of K.

Our analytical approach was restricted to a first–order approximation. Of course, one cannot expect that the shape of control domains is always reproduced to a high accuracy since the details depend on the system under consideration. Moreover one should keep in mind that in particular for large control amplitudes nonlinear contributions from the eigenvalue equation may become important, which might result in the appearance of new stability regions as well as a deformation of those domains predicted by the linear theory (cf. [15]). However, we found at least qualitative coincidence in our numerical and experimental investigations. In addition, we stress that quite similar features have been observed in different experimental realisations [16]. There, the control domain is often considered in terms of the actual system parameters and not in terms of the Lyapunov exponent of the orbit. In order to compare with our analytical result one has also to take into account the nonlinear dependence of the Lyapunov exponent on the system parameters.

Concerning the analysis of control domains we have focused on the eigenbranches associated with one positive exponent of the unstable orbit. In general, these domains may be further limited e. g. by other eigenbranches which

are connected to the stable exponents of the uncontrolled orbit and may become unstable in the course of control. Although these features are captured by our approximate analytical treatment, they depend on the particular system under consideration, since additional fit parameters enter.

Above all, the results of our analytic calculations are in reasonable agreement with numerical simulations and experimental data of an electronic circuit so that the theoretical approach captures most of the essential features.

Acknowledgement

This project of SFB 185 "Nichtlineare Dynamik" was partly financed by special funds of the Deutsche Forschungsgemeinschaft. We are indebted to F. Laeri and M. Müller for the use of their delayed feedback control device.

References

[1] R. Bellman, *Adaptive Control Processes: A Guided Tour*, (Princeton Univ. Press, Princeton, 1961).

[2] K. Pyragas, Phys. Lett. A **170**, 421 (1992).

[3] K. Pyragas and A. Tamaševičius, Phys. Lett. A **180**, 99 (1993).

[4] D. J. Gauthier, D. W. Sukow, H. M. Concannon, and J. E. S. Socolar, Phys. Rev. E **50**, 2343 (1994).

[5] J. E. S. Socolar, D. W. Sukow, and D. J. Gauthier, Phys. Rev. E **50**, 3245 (1994).

[6] K. Pyragas, Phys. Lett. A **206**, 323 (1995).

[7] S. Bielawski, D. Derozier, and P. Glorieux, Phys. Rev. E **49**, R971 (1994).

[8] T. Pierre, G. Bonhomme, and A. Atipo, Phys. Rev. Lett. **76**, 2290 (1996)

[9] W. Just, T. Bernard, M. Ostheimer, E. Reibold, and H. Benner, Phys. Rev. Lett. **78**, 203 (1997).

[10] H. Nakajima, Phys. Lett. A **232**, 207 (1997).

[11] W. Just, D. Reckwerth, J. Möckel, E. Reibold, and H. Benner, Phys. Rev. Lett. **81**, 562 (1998)

[12] J. K. Hale and S. M. Verduyn Lunel, *Introduction to Functional Differential Equations* (Springer, New York, 1993).

[13] L. Collatz, Z. angew. Math. Mech. **25/27**, 60 (1947)

[14] A. Kittel, J. Parisi, and K. Pyragas, Phys. Lett. A **198**, 433 (1995)

[15] M. E. Bleich and J. E. S. Socolar, Phys. Lett. A **210**, 87 (1996).

[16] D. Sukow, M. E. Bleich, D. J. Gauthier, and J. E. S. Socolar, Chaos **7**, 560 (1997).

[17] N. B. Tufillaro, T. Abbott, and J. Reilly, *An Experimental Approach to Nonlinear Dynamics and Chaos* (Addison–Wesley, Redwood, 1992)